Hindawi
Advances in Condensed Matter Physics
Volume 2018, Article ID 9725321, 7 pages
https://doi.org/10.1155/2018/9725321

Research Article

Thermopower Enhancement from Engineering the $Na_{0.7}CoO_2$ Interacting Fermiology via Fe Doping

Raphael Richter,[1] Denitsa Shopova,[2] Wenjie Xie,[2] Anke Weidenkaff,[2] and Frank Lechermann [3]

[1] *Institut für Technische Thermodynamik, Deutsches Zentrum für Luft- und Raumfahrt, 70569 Stuttgart, Germany*
[2] *Chemische Materialsynthese, Institut für Materialwissenschaft, Universität Stuttgart, 70569 Stuttgart, Germany*
[3] *I. Institut für Theoretische Physik, Universität Hamburg, 20355 Hamburg, Germany*

Correspondence should be addressed to Frank Lechermann; frank.lechermann@physnet.uni-hamburg.de

Received 17 January 2018; Accepted 14 March 2018; Published 23 April 2018

Academic Editor: Markus R. Wagner

The sodium cobaltate system Na_xCoO_2 is a prominent representant of strongly correlated materials with promising thermoelectric response. In a combined theoretical and experimental study we show that, by doping the Co site of the compound at $x = 0.7$ with iron, a further increase of the Seebeck coefficient is achieved. The Fe defects give rise to effective hole doping in the high-thermopower region of larger sodium content x. Originally filled hole pockets in the angular-resolved spectral function of the material shift to low energy when introducing Fe, leading to a multisheet interacting Fermi surface. Because of the higher sensitivity of correlated materials to doping, introducing adequate substitutional defects is thus a promising route to manipulate their thermopower.

1. Introduction

Selected compounds subject to strong electronic correlations display a remarkable thermoelectric response. Layered cobaltates composed of stacked triangular CoO_2 sheets are of particular interest because of their large doping range. High-thermopower above 75 μV/K has originally been detected in the Na_xCoO_2 system at larger sodium doping x~0.7 [1–4]. Even higher Seebeck coefficients and increased figure of merit have been measured for misfit cobaltates (see, e.g., [5] for a recent review). Due to the simpler crystal structure, the small-unit-cell sodium-compound system remains of key interest in view of the essential electronic structure effects underlying the pronounced thermoelectric response.

The high-thermopower region is associated with clear signatures of strong electronic correlations. Charge disproportionation [6, 7], change of Pauli-like magnetic susceptibility to Curie-Weiss-like behavior [8], and eventual onset of in-plane ferromagnetic (FM) order [7, 9–15] at $x = 0.75$ are observed. Moreover the region displays unique low-energy excitations [16].

Several theoretical works addressed the thermoelectricity of Na_xCoO_2 [17–23], ranging from applications of Heikes formula, Boltzmann-equation approaches, and Kubo-formula-oriented modeling. Correlation effects described beyond conventional density functional theory (DFT) indeed increase the thermopower. Depending on x, the oxidation state of cobalt nominally reads $Co^{(4-x)+}(3d^{5+x})$. A strong cubic crystal field establishes a Co (t_{2g}, e_g) low-spin state, and x controls the filling of the localized t_{2g} manifold. The additional trigonal crystal field splits t_{2g} into a_{1g} and e_g' levels. But the measured Fermi surface (FS) shows only a single distinct hole-like a_{1g}-dominated sheet centered around the Γ point [24, 25]. Hole pockets of mainly e_g' kind are suppressed by correlation effects [26, 27].

In this work we show that there is the possibility of engineering the interacting electronic structure of Na_xCoO_2 in view of an extra increase of the thermoelectric response. Substitutional doping of the Co site with Fe is for x~0.7 effective in shifting the e_g' hole pockets to the Fermi level ε_F. The hole doping with iron also enforces the correlation strength.

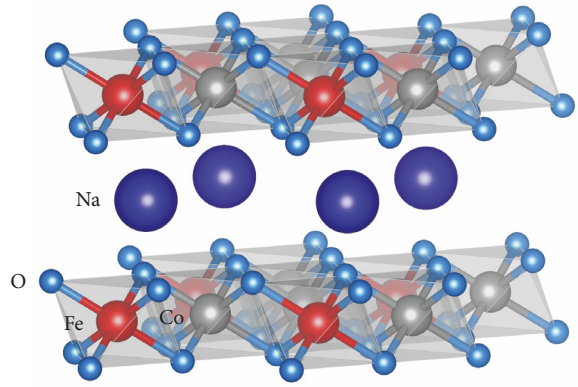

FIGURE 1: (Color online) Sketch of a Fe-doped Na_xCoO_2 structure. Note that the virtual-crystal approximation is employed in the actual calculations.

But different from the small-x region where the thermopower is found to be rather weak, for $Na_{0.7}Co_{1-y}Fe_yO_2$ the Seebeck coefficient is further enhanced. This finding paves the road for future design of thermoelectric transport in correlated materials.

2. Theoretical Approach

An advanced charge self-consistent DFT + dynamical mean-field theory (DMFT) scheme [28] is utilized. The method is based on an efficient combination of the mixed-basis pseudopotential framework [29] with continuous-time quantum Monte-Carlo in the hybridization-expansion representation [30–33] for the DMFT impurity problem. The correlated subspace consists of projected [34, 35] Co/Fe $3d(t_{2g})$ orbitals; that is, a threefold many-body treatment holds in the single-site DMFT part. The generic multiorbital Coulomb interaction is chosen in Slater-Kanamori parametrization with Hubbard $U = 5\,\text{eV}$ and Hund's exchange $J_H = 0.7\,\text{eV}$. A double-counting correction of the fully localized form [36] is used. We construct Na as well as Co pseudopotentials with fractional nuclear charge to cope with the doping scenario in a virtual-crystal approximation (VCA). Based on a primitive hexagonal cell for one formula unit Na_xCoO_2, the fractional-charged Na is in the so-called "Na2" position, that is, aside from the transition-metal position below (see Figure 1). No bilayer splitting is included. The calculations are readily extendable to more complex unit cells and geometries; however the present approach suits the purpose of rendering general qualitative statements.

For the investigation of transport, the Kubo formalism based on the correlation functions,

$$K_n = \sum_{\mathbf{k}} \int d\omega \beta^n (\omega - \mu)^n \left(-\frac{\partial f_\mu}{\partial \omega}\right) \times \text{Tr}\left[\mathbf{v}(\mathbf{k})\ A(\mathbf{k},\omega)\ \mathbf{v}(\mathbf{k})\ A(\mathbf{k},\omega)\right], \quad (1)$$

is used in the DMFT context [22, 27, 37, 38]. Here $\beta = 1/T$ is the inverse temperature, $\mathbf{v}(\mathbf{k})$ denotes the Fermi velocity calculated from the charge self-consistent Bloch bands, and f_μ marks the Fermi-Dirac distribution. To extract the k-resolved one-particle spectral function $A(\mathbf{k},\omega) = -\pi^{-1}\text{Im}\,G(\mathbf{k},\omega)$ from the Green's function G, an analytical continuation of the electronic self-energy in Matsubara space ω_n is performed via the Padé approximation. For more details we refer to [27]. This framework allows us to compute the thermopower through $S = -(k_B/|e|)(K_1/K_0)$, and the resistivity as $\rho = 1/K_0$, both beyond the constant-relaxation-time approximation.

3. Materials Preparation, Characterization, and Measurement

The powders of $Na_{0.71}Co_{1-y}Fe_yO_2$ ($y = 0$, 0.05, 0.10, and 0.15) are prepared by the Pechini method. Stoichiometric amounts of the chemicals, sodium acetate ($NaC_2H_3O_2$, 99.0%), Iron (III) nitrate nonahydrate (Sigma-Aldrich, purity 98%), cobalt acetate tetrahydrate ($(CH_3COO)_2Co{\cdot}4H_2O$, 98.0%), and citric acid ($C_6H_8O_7$, 99%, CA), are each dissolved in deionized distilled water. The calculated amount of citric acid and ingredient acetates is mandated at a molar ratio of 1.5 : 1. The precursor solution is heated in an oil bath at 65°C while stirring continuously until a uniform viscous gel (2-3 h) forms. Subsequently, ethylene glycol ($HOCH_2CH_2OH$, EG, $\rho = 1.11\,\text{g/cm}^3$) is added as a gelling agent in a molar ratio of 3 : 1 to the amount of citric acid. The gel is dried at 120°C for 4 hours and then heated in air to 300°C for 10 hours. The resulting powder is calcinated in air at 850°C for 20 hours. Densification was done in two steps: cold pressing in air (20 kN, 20 min) followed by isostatic pressing (800 kN, 1 min). Finally, the pellets are sintered for 24 hours at 900°C in air.

The samples' phase structure is identified by the Bruker D8-Advance diffractometer in Debye-Scherrer geometry with (220) Ge monochromator (Mo-Kα1, X-ray wavelength of 0.70930 Å). Seebeck coefficient and resistivity are measured simultaneously with a ZEM-3 (M10) ULVAC system, supplied with Pt electrodes, in the range $T = 30$°–350°C and 950 mBar oxygen pressure. The uncertainties for both transport properties amount to ±7%.

XRD patterns are plotted in Figure 2. For Fe substitution > 10% an impurity phase occurs. Thus the experimental study of phase-pure Fe-doped samples is here limited to $y \leq 0.1$. Note that an Fe doping of $Na_{0.63}CoO_2$ with $y \leq 0.03$ has been reported by Zhou et al. [39], but without thermoelectric characterization.

4. Correlated Electronic Structure

The $Na_{0.7}CoO_2$ electronic structure with multiorbital DMFT self-energy effects has been discussed in [27]. Electronic correlations are effective in renormalizing the low-energy t_{2g} band manifold, introducing broadening due to finite lifetime effects and shifting the occupied e_g pockets further away from the Fermi level (see top of Figure 3(a)). The single-sheet hole-like FS stems from an a_{1g} dominated band.

Replacing a fraction y of cobalt by iron introduces hole doping of the same concentration. The actual transition-metal t_{2g} filling then reads $n(t_{2g}) = 5 + x - y \equiv 5 + \tilde{x}$. We

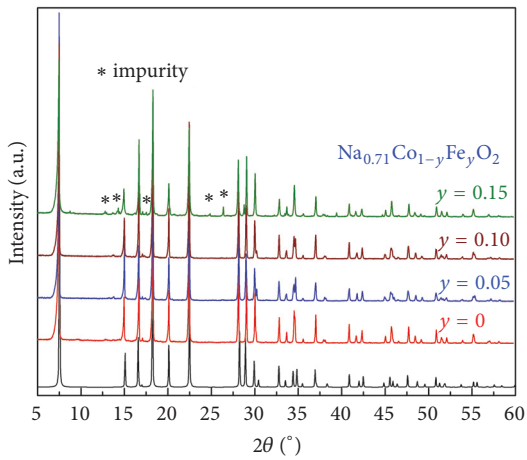

FIGURE 2: (Color online) XRD pattern of the $Na_{0.71}Co_{1-y}Fe_yO_2$ (y = 0, 0.05, 0.10 and 0.15) powder samples. Black line: reference data obtained from the ICSD database.

here employ two rather large theoretical Fe doping cases of $y = 0.25, 0.50$ to illustrate the principle effect. Because of the averaged VCA treatment, we underestimate its realistic impact and thus the lower experimental doping cases yield comparable effective physics. Figure 3 exhibits the changes of the spectral function due to hole doping y. The e_g' pockets shift towards ε_F, develop a low-energy quasiparticle (QP) resonance, and participate already for $y = 0.25$ in the FS. Since the partial bandwidth of the e_g' derived states is reduced compared to the a_{1g} one due to smaller hopping, the pocket QP resonance is rather sharp. Additionally the overall renormalization is enhanced with y and an upper Hubbard band sets in for $y = 0.50$. This strengthening of electronic correlations is not surprising since the Fe doping effectively drives $Na_{0.7}CoO_2$ again further away from the band-insulating ($x = 1$) limit. However, importantly, note that systems at a sole Na doping level x_1 and at effective doping level $\tilde{x}_1 = x_2 - y \stackrel{!}{=} x_1$ are *not* electronically identical. Let us assume lowering of the electron doping starting from $x = 0.7$ where hole pockets are shifted below ε_F. Then it was shown in [27] that for $x = 0.3$ the e_g' pockets are still suppressed at the Fermi level. But here for $\tilde{x} = 0.7 - 0.25 = 0.45$ these pockets already cross ε_F. Thus Fe doping strengthens the multiorbital transport character compared to pure Na doping.

5. Theoretical Transport

In [27] the anisotropic thermopower of sodium cobaltate at $x = 0.70, 0.75$ has been revealed using the present DFT+DMFT-based multiorbital Kubo formalism. Here we compare in Figure 4(a) the results with and without Fe doping for $Na_{0.7}CoO_2$. Quantitatively, the in-plane Seebeck values without Fe doping match the experimental data by Kaurav et al. [3]. As a proof of principles, theory documents an enhancement of the in-plane thermoelectric transport compared to the Fe-free case. For once, it may be explained by the increase of transport-relevant electron-hole asymmetry due to the emerging e_g' pockets at ε_F. A Seebeck increase because of this effect was predicted early on by model studies [20], though its realization by Fe doping was not foreseen. In addition, the small negative c-axis thermopower in Fe-free $Na_{0.7}CoO_2$ eventually changes sign for larger y. This fosters the coherency of the net thermoelectric transport.

The resistivity also increases with Fe doping and the in-plane values match our experimental data (see below). A gain of scattering because of reinforced electron correlations and appearing interband processes is to be blamed. Though the c-axis resistivity largely exceeds the in-plane one, the transport anisotropy seems still underestimated compared to measurements by Wang et al. [40].

6. Experimental Transport

In direct comparison to the theoretical data, Figure 4(b) displays the experimentally determined Seebeck coefficient. A clear observation can be extracted; namely, Fe doping gives rise to an increase of the experimental thermopower compared to the Fe-free case. But this enhancement is not of monotonic form with y and, as already remarked, the achievable phase-pure Fe content is experimentally limited to $y = 0.1$. Still, experiment verifies qualitatively the theoretical prediction on a similar quantitative level in terms of relative thermopower growth. The nonmonotonic character might result from intricate real-space effects, for example, a modification of the Co/Fe local-moment landscape, which is beyond the VCA method that was employed in theory.

The resistivity increase reported in Figure 4(b) also verifies the theoretically obtained scattering enhancement. More pronounced correlation effects, the introduced interband scattering for finite y, and/or modified vibrational properties are at the origin of this behavior. Also here, a deeper theoretical analysis beyond VCA, with additional inclusion of the phonon degrees of freedom, is in order to single out the dominate scattering mechanism.

7. Conclusions

Theory and experiment agree in the enhancement of the sodium cobaltate thermopower iron doping. This agreement may serve as a proof of principles for further engineering protocols. Our calculations for Fe-doped $Na_{0.7}CoO_2$ show that effective hole doping takes place. This shifts the originally occupied e_g'-like pockets to the Fermi level. The increased electron-hole transport asymmetry sustains an enlarged Seebeck coefficient. Iron doping also increases electronic correlations by driving the system further away from the band-insulating regime. Yet the doping is different from a nominal identical hole doping via reducing Na content. This is not of complete surprise since first, the Na atom is here an electron donor compared to the Fe atom. Second, Na ions are positioned in between the CoO_2 planes and their contribution to bonding and scattering is rather different from substitutional Fe within the planes.

It would be interesting to further analyze the engineering possibilities of the cobaltate thermopower. Strobel et al. [41]

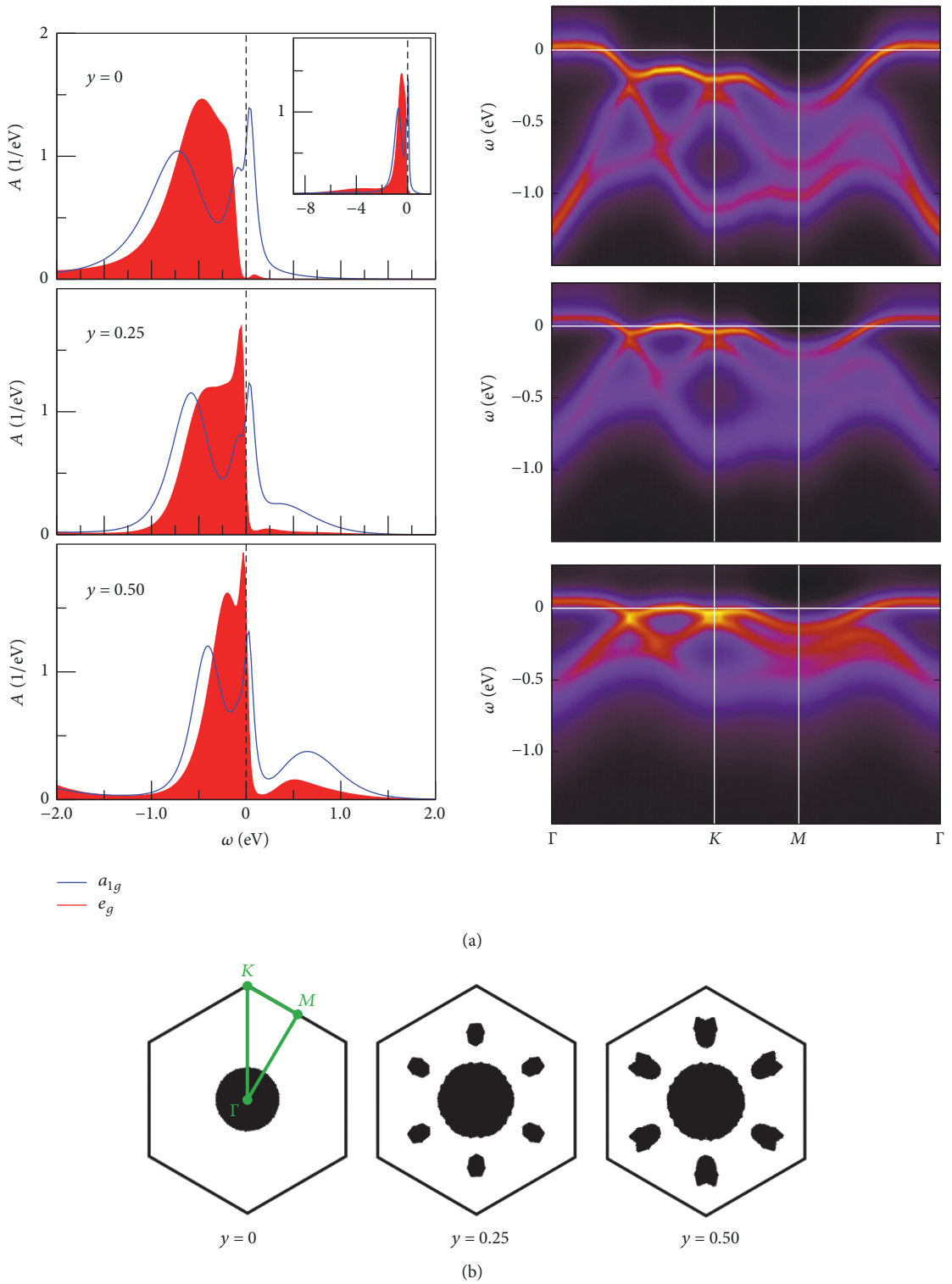

FIGURE 3: (Color online) DFT+DMFT electronic structure for $Na_{0.7}Co_{1-y}Fe_yO_2$. (a) Spectral function for different y. Left: k-integrated $A = \sum_{\mathbf{k}} A(\mathbf{k}, \omega)$ and right: k-resolved along high-symmetry lines in the Brillouin zone. (b) y-dependent FS.

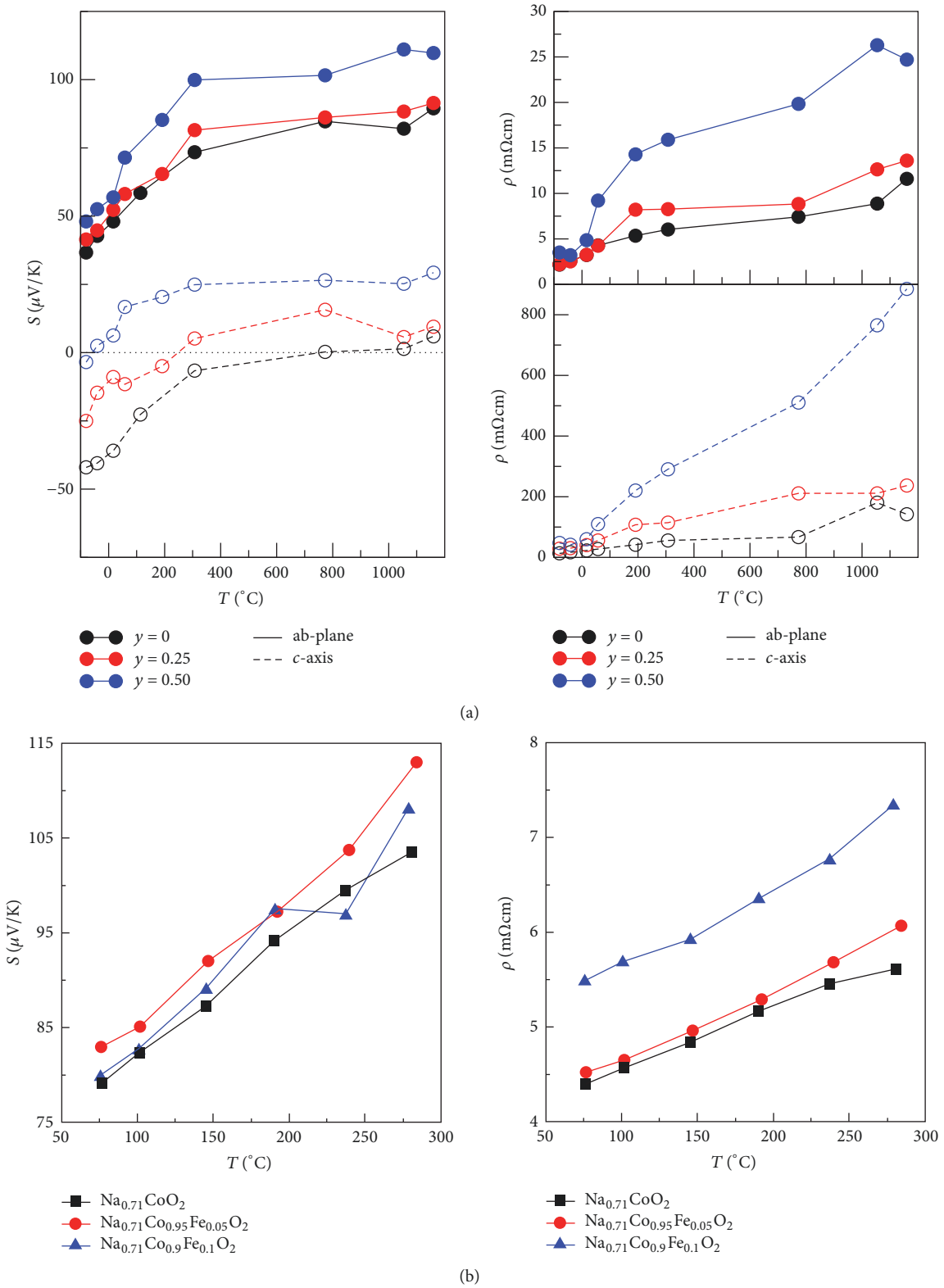

Figure 4: (Color online) Thermopower and resistivity for different Fe doping y. (a) Theoretical data from DFT + DMFT for $y = 0, 0.25, 0.50$. Solid lines: in-plane and dashed lines: along c-axis. (b) Experimental data for $y = 0, 0.05, 0.10$.

already performed experimental studies for doping with Fe-isovalent Ru and also observed a nonmonotonic thermopower increase, yet with semiconducting properties. A recent theoretical study of Sb-doped Na_xCoO_2 predicted a decrease in thermopower [42]. Generally, correlated materials are much more sensitive to doping than weakly correlated systems because of induced transfer of spectral weight. Another aspect in this regard is the nanostructuring of thermoelectric compounds [43, 44]. Research on such structuring for the case of correlated materials, combined with a tailored chemical doping, in view of increasing the figure of merit is still at its infancy. The novel field of oxide heterostructures could serve as an ideal playground.

Conflicts of Interest

The authors declare that there are no conflicts of interest regarding the publication of this paper.

Acknowledgments

The authors thank L. Boehnke, who coded the Kubo framework in their DFT + DMFT scheme, for very helpful discussions. They are indebted to D. Grieger for further theory discussions, P. Yordanov and H.-U. Habermeier for help with the transport measurements, and X. Xiao, J. Moreno Mendaza, and M. Wiedemeyer for assistance in the sample preparation. Financial support from DFG-SPP1386 and WE 2803/2-2 is acknowledged. Computations were performed at the University of Hamburg and the JURECA Cluster of the Jülich Supercomputing Centre (JSC) under Project no. hhh08.

References

[1] I. Terasaki, Y. Sasago, and K. Uchinokura, "Large thermoelectric power in single crystals," *Physical Review B: Condensed Matter and Materials Physics*, vol. 56, no. 20, pp. R12685–R12687, 1997.

[2] T. Motohashi, E. Naujalis, R. Ueda, K. Isawa, M. Karppinen, and H. Yamauchi, "Simultaneously enhanced thermoelectric power and reduced resistivity of NaxCo2O4 by controlling Na nonstoichiometry," *Applied Physics Letters*, vol. 79, no. 10, pp. 1480–1482, 2001.

[3] N. Kaurav, K. K. Wu, Y. K. Kuo, G. J. Shu, and F. C. Chou, "Seebeck coefficient of Na_xCoO_2: Measurements and a narrow-band model," *Physical Review B: Condensed Matter and Materials Physics*, vol. 79, no. 7, 2009.

[4] M. Lee, L. Viciu, L. Li et al., "Large enhancement of the thermopower in Na(x)CoO2 at high Na doping," *Nature Materials*, vol. 5, no. 7, pp. 537–540, 2006.

[5] S. Hébert, W. Kobayashi, H. Muguerra et al., "From oxides to selenides and sulfides: The richness of the CdI2 type crystallographic structure for thermoelectric properties," *Physica Status Solidi (a) – Applications and Materials Science*, vol. 210, no. 1, pp. 69–81, 2013.

[6] I. R. Mukhamedshin, H. Alloul, G. Collin, and N. Blanchard, " ^{59}Co NMR Study of the Co States in Superconducting and Anhydrous Cobaltates," *Physical Review Letters*, vol. 94, article 247602, no. 24, 2005.

[7] G. Lang, J. Bobroff, H. Alloul, G. Collin, and N. Blanchard, "Spin correlations and cobalt charge states: Phase diagram of sodium cobaltates," *Physical Review B: Condensed Matter and Materials Physics*, vol. 78, article 155116, no. 15, 2008.

[8] M. L. Foo, Y. Wang, S. Watauchi et al., "Charge ordering, commensurability, and metallicity in the phase diagram of the layered," *Physical Review Letters*, vol. 92, article 247001, no. 24, 2004.

[9] T. Motohashi, R. Ueda, E. Naujalis et al., "Unconventional magnetic transition and transport behavior in $Na_{0.75}CoO_2$," *Physical Review B: Condensed Matter and Materials Physics*, vol. 67, article 064406, no. 6, 2003.

[10] A. T. Boothroyd, R. Coldea, D. A. Tennant, D. Prabhakaran, L. M. Helme, and C. D. Frost, "Ferromagnetic in-plane spin fluctuations in Na_xCoO_2 Observed by Neutron Inelastic Scattering," *Physical Review Letters*, vol. 92, article 197201, no. 19, 2004.

[11] H. Sakurai, N. Tsujii, and E. Takayama-Muromachi, "Thermal and electrical properties of γ-NaxCoO2 ($0.70 \leq x \leq 0.78$)," *Journal of the Physical Society of Japan*, vol. 73, no. 9, pp. 2393–2396, 2004.

[12] S. P. Bayrakci, I. Mirebeau, P. Bourges et al., "Magnetic ordering and spin waves in $Na_{0.82}CoO_2$," *Physical Review Letters*, vol. 94, article 157205, no. 15, 2005.

[13] L. M. Helme, A. T. Boothroyd, R. Coldea et al., "Spin gaps and magnetic structure of Na_xCoO_2," *Physical Review B: Condensed Matter and Materials Physics*, vol. 73, article 054405, no. 5, 2006.

[14] G. J. Shu, A. Prodi, S. Y. Chu et al., "Searching for stable Na-ordered phases in single-crystal samples of γ–Na_xCoO_2," *Physical Review B*, vol. 76, article 184115, 2007.

[15] T. F. Schulze, M. Brühwiler, P. S. Häfliger et al., "Spin fluctuations, magnetic long-range order, and Fermi surface gapping in Na_xCoO_2," *Physical Review B: Condensed Matter and Materials Physics*, vol. 78, no. 20, 2008.

[16] A. Wilhelm, F. Lechermann, H. Hafermann, M. I. Katsnelson, and A. I. Lichtenstein, "From hubbard bands to spin-polaron excitations in the doped mott material," *Physical Review B: Condensed Matter and Materials Physics* Na_xCoO_2, vol. 91, no. 15, 2015.

[17] W. Koshibae and S. Maekawa, "Effects of spin and orbital degeneracy on the thermopower of strongly correlated systems," *Physical Review Letters*, vol. 87, no. 23, 2001.

[18] H. J. Xiang and D. J. Singh, "Suppression of thermopower of Na_xCoO_2 by an external magnetic field: Boltzmann transport combined with spin-polarized density functional theory," *Physical Review B*, vol. 76, article 195111, no. 19, 2007.

[19] N. Hamada, T. Imai, and H. Funashima, "Thermoelectric power calculation by the Boltzmann equation: Na xCoO2," *Journal of Physics: Condensed Matter*, vol. 19, no. 36, Article ID 365221, 2007.

[20] K. Kuroki and R. Arita, "Pudding Mold Band Drives Large Thermopower in Na_xCoO_2," *Journal of the Physical Society of Japan*, vol. 76, article 083707, 4 pages, 2007.

[21] M. R. Peterson, B. S. Shastry, and J. O. Haerter, "Thermoelectric effects in a strongly correlated model for Na_xCoO_2," *Physical Review B: Condensed Matter and Materials Physics*, vol. 76, no. 16, 2007.

[22] P. Wissgott, A. Toschi, H. Usui, K. Kuroki, and K. Held, "Enhancement of the Na_xCoO_2 thermopower due to electronic," *Physical Review B: Condensed Matter and Materials Physics*, vol. 82, no. 20, 2010.

[23] G. Sangiovanni, P. Wissgott, F. Assaad, A. Toschi, and K. Held, "Enhancement of the effective disorder potential and thermopower in Na_xCoO_2 through electron-phonon coupling," *Physical Review B: Condensed Matter and Materials Physics*, vol. 86, no. 3, 2012.

[24] M. Z. Hasan, Y.-D. Chuang, D. Qian et al., "Fermi surface and quasiparticle dynamics of $Na_{0.7}CoO_2$ investigated by angle-resolved photoemission spectroscopy," *Physical Review Letters*, vol. 92, article 246402, 2004.

[25] J. Geck, S. V. Borisenko, H. Berger et al., "Publisher's Note: Anomalous Quasiparticle Renormalization in $Na_{0.73}CoO_2$: Role of Interorbital Interactions and Magnetic Correlations," *Physical Review Letters*, vol. 99, no. 5, 2007.

[26] G. Wang, X. Dai, and Z. Fang, "Phase Diagram of Na_xCoO_2 Studied By Gutzwiller Density-Functional Theory," *Physical Review Letters*, vol. 101, no. 6, 2008.

[27] L. Boehnke and F. Lechermann, "Getting back to NaxCoO2: Spectral and thermoelectric properties," *Physica Status Solidi (a) – Applications and Materials Science*, vol. 211, no. 6, pp. 1267–1272, 2014.

[28] D. Grieger, C. Piefke, O. E. Peil, and F. Lechermann, "Approaching finite-temperature phase diagrams of strongly correlated materials: A case study for V_2O3," *Physical Review B: Condensed Matter and Materials Physics*, vol. 86, no. 15, 2012.

[29] S. G. Louie, K. Ho, and M. L. Cohen, "Self-consistent mixed-basis approach to the electronic structure of solids," *Physical Review B: Condensed Matter and Materials Physics*, vol. 19, no. 4, pp. 1774–1782, 1979.

[30] A. N. Rubtsov, V. V. Savkin, and A. I. Lichtenstein, "Continuous-time quantum Monte Carlo method for fermions," *Physical Review B: Condensed Matter and Materials Physics*, vol. 72, no. 3, 2005.

[31] P. Werner, A. Comanac, L. de' Medici, M. Troyer, and A. J. Millis, "Continuous-time solver for quantum impurity models," *Physical Review Letters*, vol. 97, no. 7, 2006.

[32] L. Boehnke, H. Hafermann, M. Ferrero, F. Lechermann, and O. Parcollet, "Orthogonal polynomial representation of imaginary-time Green's functions," *Physical Review B: Condensed Matter and Materials Physics*, vol. 84, no. 7, 2011.

[33] O. Parcollet, M. Ferrero, T. Ayral et al., "TRIQS: A toolbox for research on interacting quantum systems," *Computer Physics Communications*, vol. 196, pp. 398–415, 2015.

[34] B. Amadon, F. Lechermann, A. Georges, F. Jollet, T. O. Wehling, and A. I. Lichtenstein, "Plane-wave based electronic structure calculations for correlated materials using dynamical mean-field theory and projected local orbitals," *Physical Review B: Condensed Matter and Materials Physics*, vol. 77, no. 20, 2008.

[35] V. I. Anisimov, D. E. Kondakov, A. V. Kozhevnikov et al., "Full orbital calculation scheme for materials with strongly correlated electrons," *Physical Review B*, vol. 71, article 125119, no. 12, 2005.

[36] V. I. Anisimov, I. V. Solovyev, M. A. Korotin, M. T. Czyyk, and G. A. Sawatzky, "Density-functional theory and NiO photoemission spectra," *Physical Review B: Condensed Matter and Materials Physics*, vol. 48, no. 23, pp. 16929–16934, 1993.

[37] V. S. Oudovenko, G. Pálsson, K. Haule, G. Kotliar, and S. Y. Savrasov, "Electronic structure calculations of strongly correlated electron systems by the dynamical mean-field method," *Physical Review B: Condensed Matter and Materials Physics*, vol. 73, no. 3, 2006.

[38] X. Deng, J. Mravlje, R. Žitko, M. Ferrero, G. Kotliar, and A. Georges, "How bad metals turn good: spectroscopic signatures of resilient quasiparticles," *Physical Review Letters*, vol. 110, no. 8, 2013.

[39] T. Zhou, D. Zhang, and T. W. Button, "Substitution effects on the structural and magnetic behaviour of $Na_{0.63}CoO_2$," *Dalton Transactions*, vol. 39, no. 4, pp. 1089–1094, 2010.

[40] C. H. Wang, X. H. Chen, J. L. Luo et al., "Dimensional crossover and anomalous magnetoresistivity of superconducting Na_xCoO_2 single crystals," *Physical Review B*, vol. 71, article 224515, no. 22, 2005.

[41] P. Strobel, H. Muguerra, S. Hébert, E. Pachoud, C. Colin, and M.-H. Julien, "Effect of ruthenium substitution in layered sodium cobaltate NaxCoO2: Synthesis, structural and physical properties," *Journal of Solid State Chemistry*, vol. 182, no. 7, pp. 1872–1878, 2009.

[42] M. H. N. Assadi and H. Katayama-Yoshida, "Dopant incorporation site in sodium cobaltate's host lattice: a critical factor for thermoelectric performance," *Journal of Physics: Condensed Matter*, vol. 27, article 175504, no. 17, 2015.

[43] L. D. Hicks and M. S. Dresselhaus, "Effect of quantum-well structures on the thermoelectric figure of merit," *Physical Review B: Condensed Matter and Materials Physics*, vol. 47, no. 19, pp. 12727–12731, 1993.

[44] K. Koumoto, Y. Wang, R. Zhang et al., "Oxide Thermoelectric Materials: A Nanostructuring Approach," *Annual Review of Materials Research*, vol. 40, pp. 363–394, 2010.